



# Precipitation reduction overrides edaphic controls on nitrous oxide emissions along a soil carbon, texture and pH gradient in a cereal field

Sigrid Trier Kjær<sup>1</sup>, Peter Dörsch<sup>1</sup>

5 <sup>1</sup>Faculty of Environmental Sciences and Natural Resource Management, Norwegian University of Life Sciences, NMBU, Ås, 1433, Norway

*Correspondence to:* Sigrid Trier Kjær (sigrid.trier.kjar@nmbu.no)

**Abstract.** Nitrous oxide ( $N_2O$ ) is a potent soil-borne greenhouse gas (GHG) which increases in the atmosphere due to the widespread use of synthetic nitrogen (N) fertilisers. Soil  $N_2O$  emissions are intrinsically controlled by soil moisture and edaphic properties such as soil organic carbon (SOC) content, texture and pH. With a future climate projected to increase frequency and severity of droughts in northern Europe, understanding how these factors interact to affect  $N_2O$  emissions is critical for predicting climate feedbacks. In this study, we investigated  $N_2O$  emissions along a hillslope gradient in an agricultural field in southeast Norway, characterised by increasing SOC and clay content and decreasing pH from top to bottom. Eight rainout shelters were installed along the hillslope, nominally reducing precipitation by 49%.  $N_2O$  emissions were measured weekly using static chambers over two years during the snow-free period. In the first year,  $N_2O$  emission measurements started two months after fertilisation and covered a four-month period, which included episodes of heavy rainfall; during this time, we found no effect of precipitation reduction or edaphic factors on emission rates. In the second year, reduced precipitation significantly decreased  $N_2O$  emissions (~25%). Under ambient precipitation, cumulative  $N_2O$  emissions were positively correlated with SOC content and showed weak negative and positive trends with soil pH and clay content, respectively. No significant correlations were found in plots with reduced precipitation. Altogether, our findings illustrate that soil physicochemical controls on  $N_2O$  emissions depend on the interaction between soil properties and climate. This has consequences for parameterising process-based  $N_2O$  models driven by soil properties and weather and calls for more in-depth studies on interdependencies of edaphic and climatic drivers of  $N_2O$  emissions.

## 25 1 Introduction

Nitrous oxide ( $N_2O$ ) dominates the greenhouse gas (GHG) footprint of crop production and emissions have increased significantly since the industrialisation of agriculture.  $N_2O$  is a potent and long-lived GHG with a global warming potential 273 times that of carbon dioxide ( $CO_2$ ) over a 100-year timescale (IPCC, 2023). Moreover, after successfully banning chlorofluorocarbons,  $N_2O$  has become the most important ozone-depleting substance in the stratosphere (Ravishankara et al.,



30 2009). With the ongoing intensification of global food production based on synthetic fertiliser use, global  $\text{N}_2\text{O}$  emissions continue to grow, and the atmospheric mixing ratio of  $\text{N}_2\text{O}$  has risen by more than 20% from 1750 to 2018 (Tian et al., 2020).

While  $\text{N}_2\text{O}$  contributes to climate change, its production and consumption in soils are strongly driven by soil moisture and temperature. According to climate predictions for Norway and much of Europe, the future climate is expected to experience 35 more frequent and severe summer droughts, along with increased and more extreme precipitation (Wong et al., 2011; Hanssen-Bauer et al., 2017; Zhu and Siebert, 2024). Soil moisture and oxygen ( $\text{O}_2$ ) levels strongly control  $\text{N}_2\text{O}$  turnover in the soil (Firestone et al., 1979). For instance, nitrification requires  $\text{O}_2$  to oxidise ammonium ( $\text{NH}_4^+$ ) to nitrate ( $\text{NO}_3^-$ ) and becomes more active at low soil moistures (WFPS < 60%) when  $\text{O}_2$  diffuses readily into the soil. Conversely, high soil moistures (WFPS > 60%) support anoxic conditions, inducing denitrification which reduces  $\text{NO}_3^-$  to dinitrogen ( $\text{N}_2$ ) with 40  $\text{N}_2\text{O}$  as an intermediate (Firestone, 1982; Davidson, 1993).

Fluctuations in soil moisture can trigger hot moments of increased  $\text{N}_2\text{O}$  emissions, especially when dry soils are rewetted (Butterbach-Bahl et al., 2013; Barrat et al., 2021). Although drying-rewetting cycles in soils experiencing drought or reduced precipitation can result in transiently large  $\text{N}_2\text{O}$  emissions, seasonal  $\text{N}_2\text{O}$  emissions are likely smaller than in wet soils receiving more precipitation (Borken and Matzner, 2009). In general, reduced precipitation tends to decrease  $\text{N}_2\text{O}$  emissions 45 (Hartmann and Niklaus, 2012; Homyak et al., 2017; Li et al., 2020), the extent of which depends on the magnitude and duration of precipitation change. Meta-analyses of precipitation manipulation experiments revealed that reduced precipitation decreases  $\text{N}_2\text{O}$  emissions, although with variable effects, ranging from 7.1% (Yang et al., 2022) to 31% (Li et al., 2020) and 38.5% (Wu et al., 2022) compared to controls with ambient precipitation.

$\text{N}_2\text{O}$  production and consumption are also influenced by soil physicochemical properties. Soil organic matter (SOM) is an 50 important factor supporting heterotrophic microbial activity, N mineralisation and  $\text{O}_2$  consumption in the soil matrix (Li et al., 2005; Jäger et al., 2011; Rummel et al., 2020). SOM also increases the soil's water holding capacity with consequences for soil redox conditions (Nemes et al., 2005). Once soils become anoxic, soil organic carbon (SOC) and its degradation products fuel anoxic respiration with N oxyanions ( $\text{NO}_3^-$ ,  $\text{NO}_2^-$ ) as terminal electron acceptors (i.e. denitrification). Furthermore, the decomposition of labile organic carbon (C) can create anoxic zones, promoting hotspots for denitrification 55 (Schlüter et al., 2025).

Another important soil physicochemical property is soil texture which affects soil moisture and SOC content (Kaiser et al., 1996; Keiluweit et al., 2018; Li et al., 2024; Kjær et al., 2026a). Fine-textured soils have higher water retention capacity compared to coarse-textured soils and are more prone to developing anoxia due to slower diffusion of  $\text{O}_2$  from the atmosphere (Pihlatie et al., 2004). At the same time, soil-borne  $\text{N}_2\text{O}$  lingers longer in the soil, increasing the opportunity for 60 reduction to  $\text{N}_2$ . Additionally, SOC is stabilised by clay, resulting in generally greater C contents in clayey soils (Six et al., 2002a) due to physical protection of SOC from decomposition which, however, is susceptible to release by drying-rewetting and may fuel  $\text{N}_2\text{O}$  production (Harrison-Kirk et al., 2013). Clay content covaries with other soil chemical properties which potentially influence  $\text{N}_2\text{O}$  turnover; for example, clay particles have a higher cation exchange capacity compared to sand,



allowing  $\text{NH}_4^+$  to bind more effectively and making  $\text{NH}_4^+$  less available for nitrification, thus reducing nitrification derived  
65  $\text{N}_2\text{O}$  emissions and  $\text{NO}_3^-$  supply to denitrification (Yu et al., 2019). Therefore, clay may have adverse effects on  $\text{N}_2\text{O}$  production and consumption.

Another important edaphic parameter for net  $\text{N}_2\text{O}$  production in soils is pH. It is widely recognised that pH affects the final reduction step of denitrification, with lower pH (typically pH 5–8 in agricultural soils) increasing  $\text{N}_2\text{O}$  production relative to  
70  $\text{N}_2$  production (Stevens et al., 1998; Bakken et al., 2012). This is because acidic conditions impair the functioning of  $\text{N}_2\text{O}$  reductase (*NosZ*), which converts  $\text{N}_2\text{O}$  to  $\text{N}_2$ , leading to an increase of the  $\text{N}_2\text{O}$  product ratio of denitrification (Bakken et al., 2012).

Understanding the interactions between soil physicochemical properties and climatic conditions is critical for the  
75 parameterisation of process models predicting  $\text{N}_2\text{O}$  emissions and their responses to future environmental changes (Ge et al., 2024). While previous studies have explored the effects of reduced precipitation on  $\text{N}_2\text{O}$  emissions, there remain gaps in our understanding of how these effects interact with soil properties such as SOC, clay content and pH in cultivated soils.

The aim of this study was to investigate how precipitation regime interferes with the variability of SOC, clay content and pH common in cultivated upland soils in controlling  $\text{N}_2\text{O}$  emissions. We measured  $\text{N}_2\text{O}$  emission in paired plots under rainout  
80 shelters, that nominally reduced precipitation by 49%, and in control plots with ambient precipitation. The plots were cultivated identically and located along a natural gradient of SOC, clay and pH. We measured  $\text{N}_2\text{O}$  fluxes weekly throughout two growing seasons using manual chambers.

## 2 Materials and Methods

### 2.1 Field site and rainout shelters

The field experiment was conducted along a 62 m-long gentle (1.8%) hillslope on the experimental farm “Kjerringjordet” at the Norwegian University of Life Sciences in Ås, Norway (59°39'44.8"N, 10°45'48.3"E). The hillslope features a natural  
85 gradient with increasing SOC and clay and decreasing pH from top to bottom, and the soil type changes from loam to clay loam downslope. The slope has a north-east to south-west orientation with north-west-facing aspect. To the south, there is a treeline that shades the plots at the bottom of the slope for most of the day during the winter months.

Eight 2.5 × 2.5 m rainout shelters were installed along the hillslope (Fig. S1). The rainout shelters were custom-made as described in Kundel et al. (2018). Each shelter had nine 90° V-profiles, which were 2.5 m long and 96 mm wide. With nine  
90 V-profiles, 49% of the precipitation should be excluded from the plot. We installed a rain gutter on each shelter to ensure that the precipitation was diverted away from the plot. Uphill from each rainout shelter, a control plot with ambient precipitation was established resulting in a total of 16 plots. Soil volumetric water content (VWC) and temperature were measured at a depth of 5 cm in 13 of the 16 plots using time domain reflectometry (TDR, Decagon Em50). Based on the individual bulk density measured in each plot (n = 3) and a standard particle density of 2.65 g cm<sup>-3</sup>, plot-wise water filled



95 pore space (WFPS) was calculated. Precipitation data were obtained from a nearby weather station at NMBU, Ås (59°39'37.8"N, 10°46'54.5"E) (Wolff and Grimenes, 2024; Wolff, 2025).

The experiment was conducted from June 2023 until November 2024 (Table 1). The field was managed using conventional agricultural practices. It was harrowed in spring, sown to barley (*Hordeum vulgare*, cultivar Salome) with a seeding rate of 210 kg ha<sup>-1</sup> and fertilised with 121 kg N ha<sup>-1</sup> in 2023 and 132 kg N ha<sup>-1</sup> in 2024 (YaraMila, NPK 22-3-10). Biomass samples 100 for determining yield were collected by hand. In each plot, rows of barley were cut to a length of one metre under the rainout shelters and in the control plots. The distance between rows was 12.5 cm and yields were upscaled to the hectare. Rainout shelters were removed from the field just before the first snowfall and moved back again when snow was thawed (Table 1).

105 **Table 1: Timeline of field activities during the experimental period for the first year (2023) and the second year (2024). Gas measurements continued beyond the removal of rainout shelters in the second year**

	Sowing and fertilisation	Harvest	Rainout shelters	Gas measurements
Year 1: 2023	-	12.9	26.6 to 26.10	28.6 to 24.10
Year 2: 2024	7.5	28.8	21.3 to 14.11	2.3 to 26.11

## 2.2 Field N<sub>2</sub>O measurements

N<sub>2</sub>O emission rates were measured weekly from June to October 2023 and March to November 2024 by manual static 110 chambers (Table 1). Frames with a water lock were installed in the middle of the rainout shelters and in a similar position in the control plots. N<sub>2</sub>O emission rates were estimated from four samples drawn by syringe from the chambers for 30-60 minutes chamber deployment and transferred to pre-evacuated 10 ml glass vials with crimp sealed butyl rubber septa. Measurements were carried out between 11 a.m. and 2 p.m. Concentrations of N<sub>2</sub>O, CO<sub>2</sub> and CH<sub>4</sub> in the vials were determined by a multi-column, multi-detector gas chromatograph (GC; Agilent 7890A) with two columns (PoraPLOT Q 115 column and Molesieve column) and three detectors (TCD, FID and ECD) as described by Kjær et al. (2026b). Standard mixtures (AGA, Norway) were measured alongside the vials for calibration. CO<sub>2</sub> was used to quality-check N<sub>2</sub>O measurements. Emission rates were fitted to a linear regression to estimate the emission rate from the change in concentration, and fluxes were cumulated using linear interpolation with the R package *DescTools* (version 0.99.54; Signorell and Ekstrom, 2024).

## 120 2.3 Ancillary variables

Two soil samples (0-20 cm) were taken monthly from each plot (during the snow-free period) and pooled, before extracting NO<sub>3</sub><sup>-</sup> and NH<sub>4</sub><sup>+</sup> in a 1M KCl solution, followed by filtration and spectrophotometry (Doane and Horwáth, 2003; Krom,



1980). Gravimetric soil moisture was determined in the same samples by drying. An extra set of soil samples for determining soil properties were collected on 24 October 2023. In each plot, five samples were taken from a depth of 0-20 cm and mixed.

125 Each sample was analysed for total C and N, soil texture and pH (Table 2). Total C and N contents and stable isotope ratios ( $\delta^{13}\text{C}$  and  $\delta^{15}\text{N}$ ) were measured by an element analyser (FlashEA 1112 HT, Thermo Fisher Scientific) coupled to an isotope ratio mass spectrometer (Delta<sup>plus</sup>XP, Thermo Finnigan). Soil texture was determined using the pipette method (Krogstad et al., 1991; Elonen, 1971) and pH was measured in water in autumn 2023 and spring 2024. pH was remeasured in 2024 because an adjacent field was limed in winter 2023/2024 and, as the snow thawed, some lime was transported close to our field. The pH increased by  $0.18 \pm 0.12$  from 2023 to 2024 (Table 2). Volumetric samples for determining porosity and bulk density were taken in triplicate steel cylinders ( $100 \text{ cm}^3$ ) at a depth of 10-15 cm in each plot at the end of the experiment (spring 2025). Field capacity was defined as the water content at  $-33 \text{ kPa}$ . Volumetric water content (VWC) at field capacity was calculated from the mass difference between soil cores equilibrated at  $33 \text{ kPa}$  and oven-dried samples and normalised by the cylinder volume ( $n = 3$ ).

135



**Table 2: Soil properties for control and rainout shelter plots along the hillslope (m from hilltop). Plot names are A to H and \* indicates plots that were equipped with a TDR sensor. Given are soil organic carbon (SOC, mg g dry weight<sup>-1</sup>), C:N ratio, clay (%), silt (%), sand (%), pH (measured in both 2023 and 2024), bulk density (g cm<sup>-3</sup>) and volumetric water content at field capacity (VWC at FC, %). Samples were taken from a depth of 0-20 cm for all variables except bulk density and VWC at field capacity which were determined at a depth of 10-15 cm.**

Metres from hilltop	Plot	Treatment	SOC <sup>a</sup> mg g <sup>-1</sup>	C:N <sup>a</sup> ratio	Clay <sup>a</sup> %	Silt <sup>a</sup> %	Sand <sup>a</sup> %	pH <sup>a</sup> 2023	pH 2024	Bulk density g cm <sup>-3</sup>	VWC at FC %
0	A *	Control	28.3	11.2	24	39	37	5.92	6.15	1.16 ± 0.03	32 ± 0.6
2		* Rainout shelter	28.3	10.8	24	42	34	5.93	6.11	1.24 ± 0.03	33.4 ± 0.3
8	B *	Control	27.3	10.5	25	38	37	6.11	6.10	1.28 ± 0.02	33.4 ± 0.6
10		Rainout shelter	28.1	10.4	25	37	38	6.11	6.13	1.18 ± 0.05	32.1 ± 1.8
16	C *	Control	29.9	10.7	28	36	36	5.96	5.99	1.22 ± 0.03	31.5 ± 0.4
18		* Rainout shelter	29.6	10.8	24	43	33	5.83	5.96	1.18 ± 0.04	30.6 ± 0.8
24	D	Control	28.2	10.7	24	39	36	5.89	6.10	1.17 ± 0.02	30.5 ± 0.4
26		Rainout shelter	29.1	11.0	28	36	36	5.86	6.14	1.24 ± 0.02	32.7 ± 0.6
32	E *	Control	29.5	10.9	24	41	34	5.90	6.05	1.22 ± 0.01	32.8 ± 0.5
34		* Rainout shelter	28.8	11.1	28	38	34	5.92	6.11	1.23 ± 0.02	30.9 ± 0.1
44	F *	Control	30.5	10.9	26	38	36	5.86	5.98	1.24 ± 0.05	32.6 ± 0.8
46		* Rainout shelter	31.7	11.2	29	35	36	5.83	5.91	1.26 ± 0.04	32.7 ± 0.6
52	G *	Control	36.1	11.2	30	36	33	5.44	5.88	1.19 ± 0.02	33.4 ± 0.6
54		* Rainout shelter	37.2	11.3	32	35	33	5.64	5.86	1.13 ± 0.02	32.6 ± 1.1
60	H *	Control	38.1	11.3	32	36	32	5.55	5.92	1.15 ± 0.01	34.4 ± 0.3
62		* Rainout shelter	37.7	11.4	34	34	32	5.62	5.90	1.12 ± 0.04	33.4 ± 1.3

<sup>a</sup> from Kjær et al. (2026a)



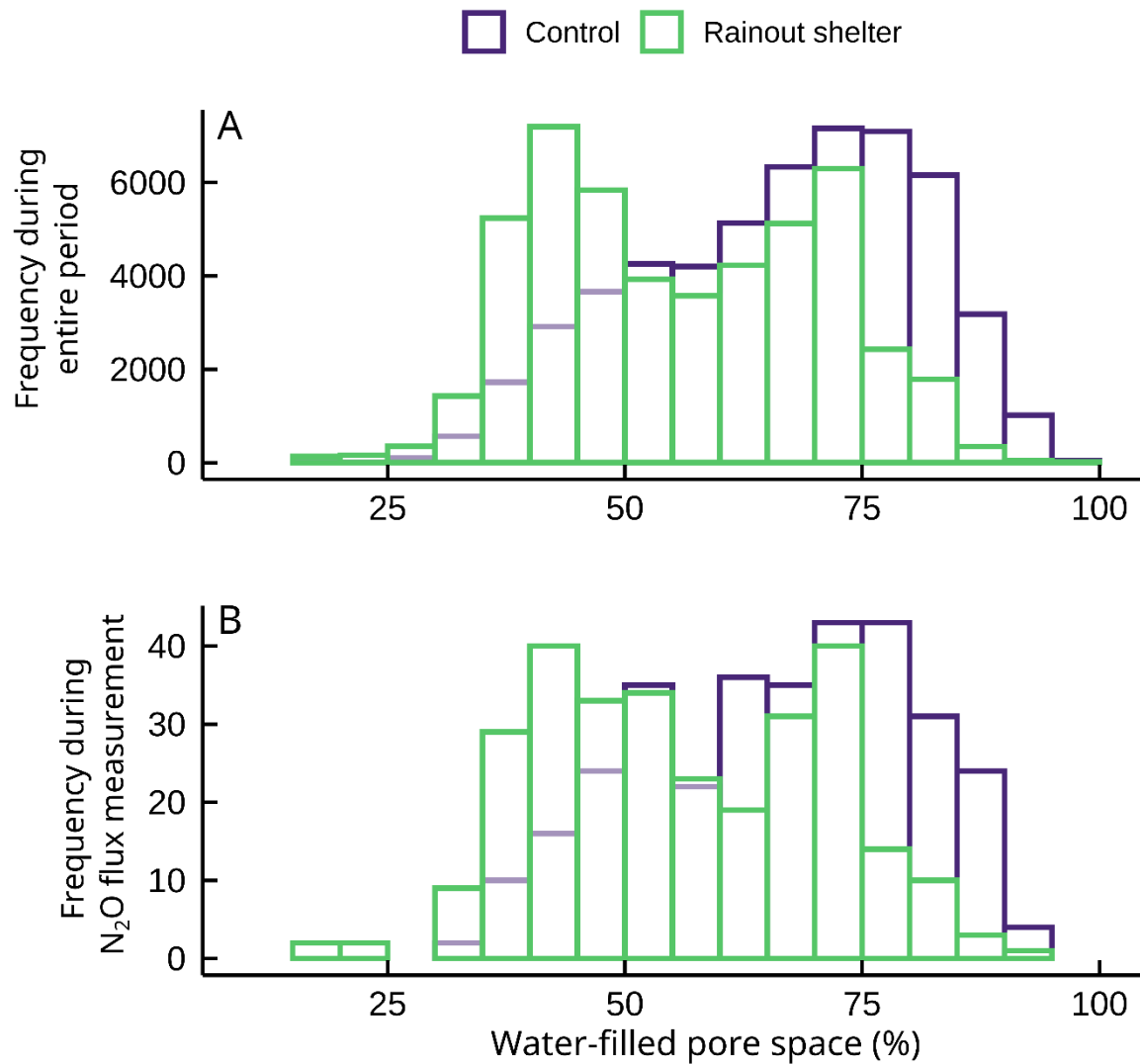
## 2.4 Statistics

A linear mixed-effects model was used to compare  $\text{N}_2\text{O}$  emission rates and mineral N ( $\text{NO}_3^-$  and  $\text{NH}_4^+$ ) contents between rainout shelter and control plots. We used the lmer and lmerTest packages with the plots along the gradient as pseudo-replicates to test the difference in precipitation treatment, accounting for repeated measurements on the same plots. Differences in cumulative  $\text{N}_2\text{O}$  emissions and dry matter yield (DMY) between treatments were tested using a non-parametric Wilcoxon rank-sum test and unpaired t-tests, respectively. These tests were chosen because cumulative  $\text{N}_2\text{O}$  emissions were not normally distributed, while yield data were approximately normal (Shapiro-Wilk tests). Levene's tests confirmed similar variances across treatments in both datasets. Relationships between cumulative  $\text{N}_2\text{O}$  emissions and soil properties (SOC, pH, clay content and bulk density) were analysed using linear regression, with regression coefficients,  $R^2$  values and p-values reported. Statistical significance was set to  $p < 0.05$ . All statistical analyses were performed using R version 4.5.1 (R Core Team, 2025).

## 3 Results

### 155 3.1 Impact of rainout shelters on soil moisture distribution

Water-filled pore space (WFPS) values, calculated from plot-specific bulk densities and continuously logged volumetric water contents from periods with rainout shelters and gas measurements (excluding the winters), were higher in the control plots than under the rainout shelters. This confirms that the shelters effectively reduced soil moisture (Fig. 1). The frequency distribution of WFPS in the rainout shelter plots was bimodal, with two maxima at 35–50% and 65–75% WFPS (Fig. 1A). 160 By contrast, the distribution of WFPS in the control plots was unimodal and left-skewed with a maximum at 65–85% WFPS. When plotting WFPS frequency distribution for soil moistures measured during flux measurements (Fig. 1B), the distribution closely resembled that of the entire experimental period, particularly for the rainout shelter plots, suggesting that flux measurements represented the rainout effect well.



165

Figure 1: Frequency distribution of water-filled pore space values (WFPS, %) for control plots (purple) and rainout shelter plots (green). (A) WFPS frequency distribution based on hourly measurements during the entire experimental period, from the installation of rainout shelters until the end of gas measurements for both years. (B) WFPS frequency distribution based on average WFPS measurements taken between 11 a.m. and 2 p.m. in each plot during dates of flux sampling. Volumetric water content was measured in 13 out of the 16 plots at a depth of 5 cm, and WFPS was calculated using measured bulk density and a standard particle density

170

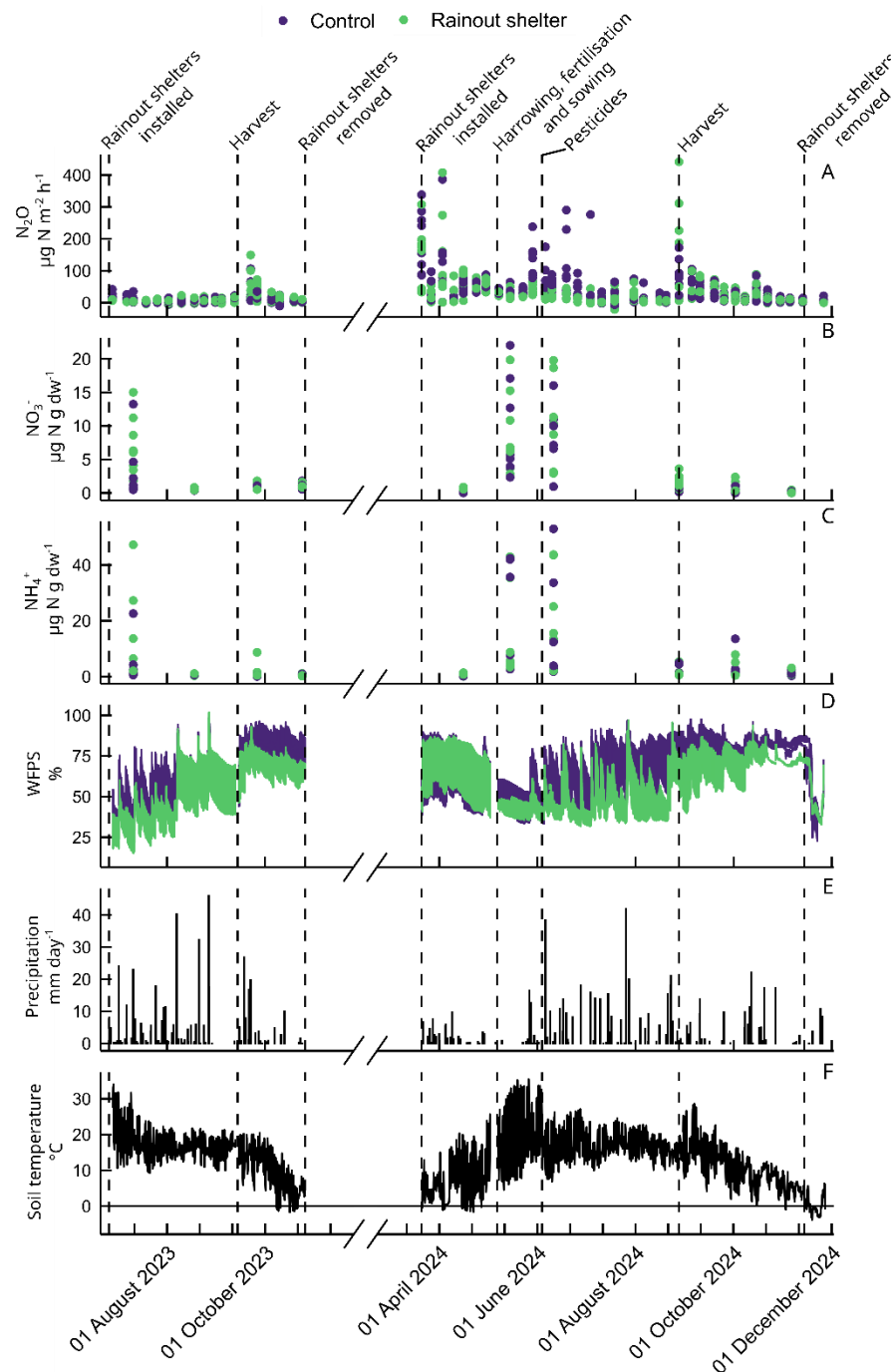


### 3.2 Differences between years

In the first year,  $\text{N}_2\text{O}$  emission measurements started in June right after installing the rainout shelters, about two months after 175 sowing and fertilisation. Emission rates ranged from  $-10.4$  to  $149.6 \mu\text{g N m}^{-2} \text{ h}^{-1}$  with a median of  $5.6$  and no significant differences between plots under rainout shelters and control plots ( $p = 0.8$ , linear mixed-effect model; Fig. 2A). In the second year, higher emission rates were measured in the control plots ( $p = 0.005$ , linear mixed-effect model). Large  $\text{N}_2\text{O}$  emission rates were measured after spring thaw when temperatures were still low, and in autumn right after harvest (Fig. 2A).  $\text{N}_2\text{O}$  emission rates ranged from  $-21.1$  to  $441.4 \mu\text{g N m}^{-2} \text{ h}^{-1}$  with a median of  $22.3$ , which was clearly higher than observed in the 180 first year. After harvest, larger emission rates were measured under the rainout shelters than in control plots. We did not observe a clear emission response to fertilisation, but some larger emission rates were detected during summer following precipitation events, especially in the control plots.

Mineral N ( $\text{NO}_3^-$  and  $\text{NH}_4^+$ ) contents at 0-20 cm depth were highest in spring and early summer (Fig. 2B and 2C), without 185 showing a significant difference between the rainout shelter and control plots ( $p = 0.29$  and  $0.67$  for  $\text{NO}_3^-$  and  $\text{NH}_4^+$ , respectively, Fig. S2). We tested differences in mineral N content across both years using a linear mixed-effects model.

Overall, rainout shelters reduced soil moisture (Fig. 2D). However, there were times when high precipitation (Fig. 2E) caused soil moisture in the rainout shelter plots to be similar to or even higher than in the control plots. This occurred in the first year, after two extreme precipitation events in August, when more than 40 mm of precipitation fell within 24 hours (Wolff and Grimenes, 2024); and again in the spring of the second year during snowmelt. The lowest WFPS values were 190 measured at the beginning of the first year, following a drought period prior to the start of the experiment (Wolff and Grimenes, 2024). Similarly, low WFPS was recorded at the end of the second year when temperatures dropped below the freezing point, because time domain reflectometry (TDR) loggers do not detect frozen water (Fig. 2D and 2F).

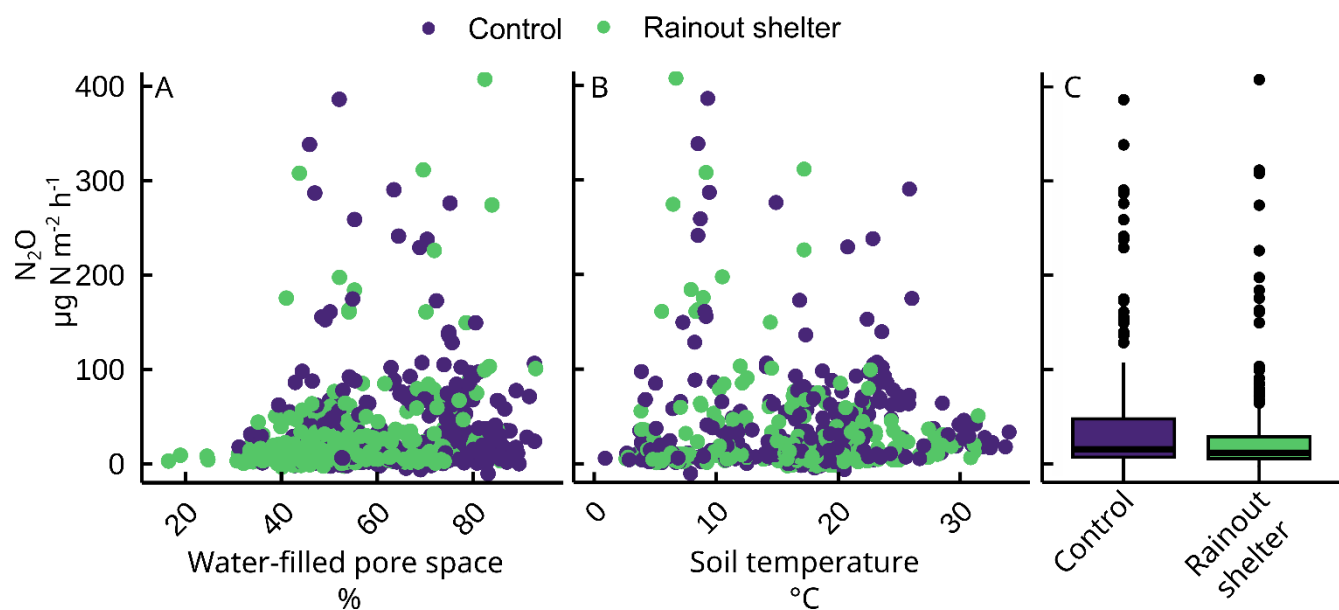


195 **Figure 2:  $\text{N}_2\text{O}$  emission rates (single plot values) and ancillary variables in control plots (purple) and rainout shelter plots (green).** (A)  $\text{N}_2\text{O}$  emission rates, (B) and (C) extractable soil  $\text{NO}_3^-$ -N and  $\text{NH}_4^+$ -N per g dry weight soil collected at a depth of 0-20 cm, (D) water-filled pore space (WFPS) calculated from volumetric water content, (E) precipitation ( $\text{mm day}^{-1}$ ) obtained from a nearby weather station (Wolff and Grimenes, 2024; Wolff, 2025) and (F) mean soil temperature measured at a depth of 5 cm. Dashed vertical lines indicate key management events



## 200 3.3 Variation in daily emission rates

N<sub>2</sub>O emission rates were largest at WFPS values between 41% and 82% (Fig. 3A) and temperatures below 10°C (Fig. 3B). High flux rates (>100  $\mu\text{g N m}^{-2} \text{h}^{-1}$ ) originated primarily from spring in the second year, when soil moisture was high and temperature was low (Fig. 2D and 2F). Large N<sub>2</sub>O emission rates were also observed when temperatures were between 15°C and 25°C, particularly in the control plots. As shown in Fig. 1, rainout shelter plots had fewer N<sub>2</sub>O measurements with 205 WFPS values exceeding 75%, thus reducing high emission fluxes during wet conditions. This can also be seen from Fig. 3A, even though some rainout shelter plots still exhibited high N<sub>2</sub>O emission rates under conditions of very high WFPS (>80%).



210 **Figure 3:** Relationship between N<sub>2</sub>O emission rates ( $\mu\text{g N m}^{-2} \text{h}^{-1}$ ) and (A) water-filled pore space (WFPS, %) and (B) soil temperature (°C). Both WFPS and soil temperature were measured at a depth of 5 cm. Data points represent individual measurements with colours indicating either control plots (purple) or rainout shelter plots (green). (C) Boxplot of N<sub>2</sub>O emission rates shown in (A) and (B) with median, interquartile range and whiskers indicating variability outside the upper and lower quartiles

## 3.4 Cumulative N<sub>2</sub>O emissions and yield

Cumulative N<sub>2</sub>O emissions cannot be compared between the years because of different measurement periods (Table 1). In 215 the first year, cumulative N<sub>2</sub>O emissions were smaller in five out of the eight rainout shelter plots compared with their adjacent control plots (Fig. 4A). However, the differences between plots were small, and a non-parametric Wilcoxon rank-sum test showed no significant difference in cumulative N<sub>2</sub>O emission between rainout shelter and control plots (Fig. 4C,  $p = 0.645$ ). In the second year, the differences in cumulative N<sub>2</sub>O emissions between treatments were more pronounced (Fig. 4B). Six out of eight rainout shelter plots had smaller emissions than the adjacent control plots. When testing the difference 220 across all plots, cumulative N<sub>2</sub>O emissions in the rainout shelter plots were  $1.94 \pm 0.62 \text{ kg N ha}^{-1}$  ( $\pm\text{SD}$ ) and significantly smaller than the  $2.58 \pm 0.43 \text{ kg N ha}^{-1}$  ( $\pm\text{SD}$ ) in the control plots (Fig. 4D,  $p = 0.038$ , Wilcoxon rank-sum test).

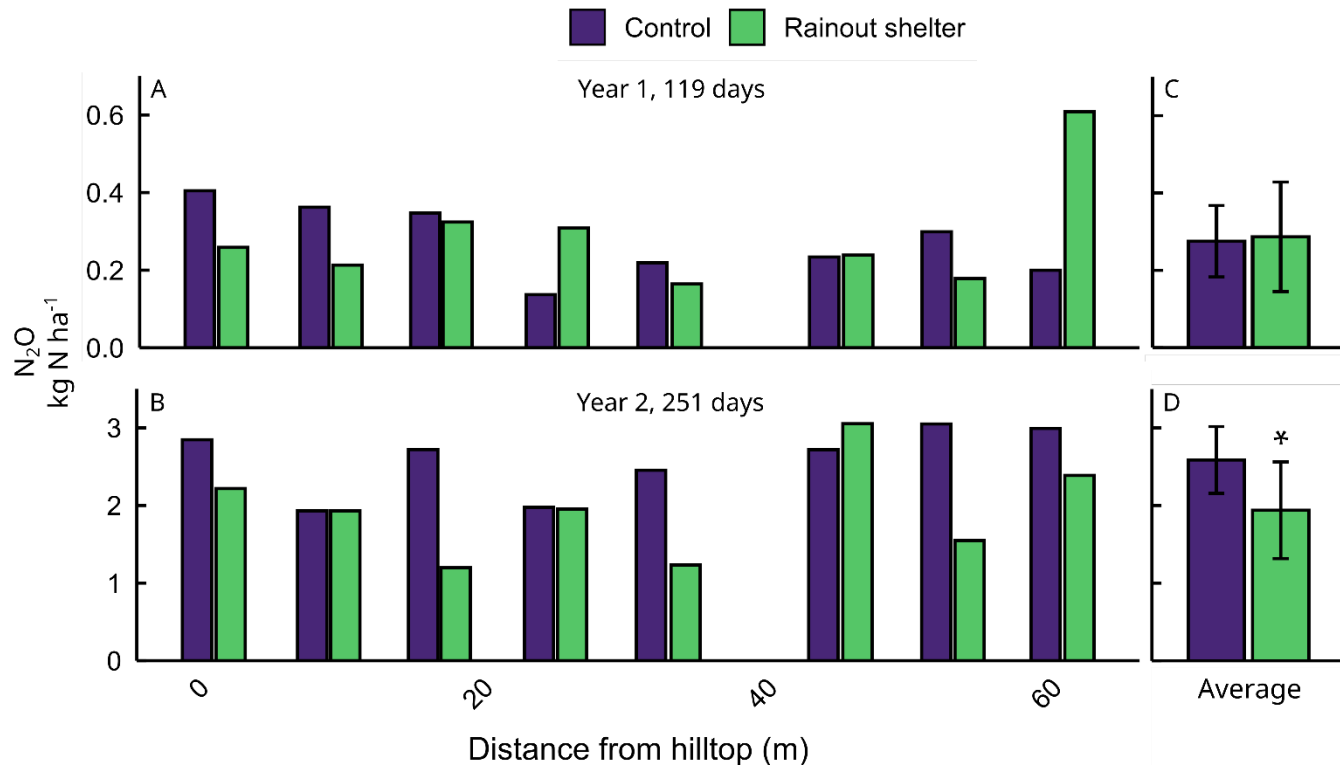


**Figure 4: Cumulative N<sub>2</sub>O emissions (kg N ha<sup>-1</sup>) along the transect calculated by linear interpolation for the first year (Year 1, 119 days: A and C) and the second year (Year 2, 251 days: B and D). A and B show cumulative N<sub>2</sub>O emissions as a function of distance from the hilltop (m) for control plots (purple) and rainout shelter plots (green). C and D present averages  $\pm$  standard deviation for control plots (purple) and rainout shelter plots (green) across the hillslope. The asterisk denotes significance ( $p < 0.05$ ) between treatments**

225

The rainout treatment had no significant effect on dry matter yields (DMY) in either year ( $p = 0.071$  and  $0.435$  for the first and the second year, respectively; Fig. 5) but showed a tendency towards lower yields under rainout shelters.

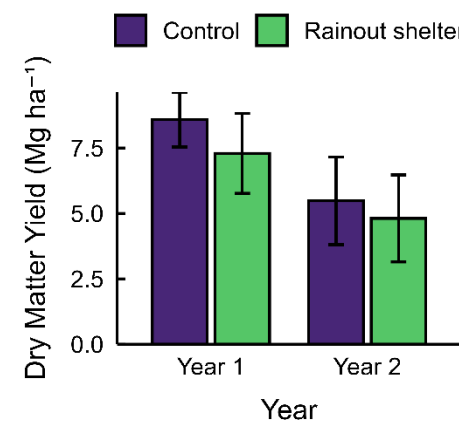


**Figure 5: Mean dry matter yield (DMY) of barley for the first (Year 1) and the second (Year 2) experimental year (Mg ha<sup>-1</sup>). Bars represent the average DMY  $\pm$  standard deviation (Mg ha<sup>-1</sup>) for control plots (purple) and rainout shelter plots (green)**

230



### 3.5 Soil properties and cumulative N<sub>2</sub>O emissions

235 Soil properties varied along the hillslope (Table 2) with SOC and clay content increasing and pH decreasing toward the bottom of the slope. We tested the relationships between cumulative N<sub>2</sub>O emissions and soil properties separately for rainout shelter and control plots for both experimental years. In the first year, no significant correlations with edaphic parameters emerged for either treatment (control:  $p = 0.53$  (SOC),  $p = 0.46$  (pH),  $p = 0.78$  (clay) and  $p = 0.48$  (bulk density); rainout shelters:  $p = 0.22$  (SOC),  $p = 0.19$  (pH),  $p = 0.31$  (clay) and  $p = 0.24$  (bulk density); data not shown). In the second year, 240 cumulative N<sub>2</sub>O emissions in the control plots were positively correlated with SOC content (Fig. 6A,  $p = 0.04$ ), weakly negatively with soil pH (Fig. 6B;  $p = 0.08$ ) and weakly positively with clay content (Fig. 6C,  $p=0.06$ ). This pattern disappeared when analysing cumulative emissions in rainout shelter plots. Here, neither SOC ( $p = 0.66$ ), soil pH ( $p = 0.62$ ) nor clay ( $p = 0.49$ ) was near to significance. Although correlations with pH and clay content in the control plots were not significant, they showed near-significant trends. SOC, pH, and clay content were all significantly correlated with each other 245 ( $p < 0.05$ ), making it difficult to disentangle their individual effects on cumulative N<sub>2</sub>O emissions. Bulk density showed no correlation with cumulative N<sub>2</sub>O emissions for either treatment (Fig. 6D).

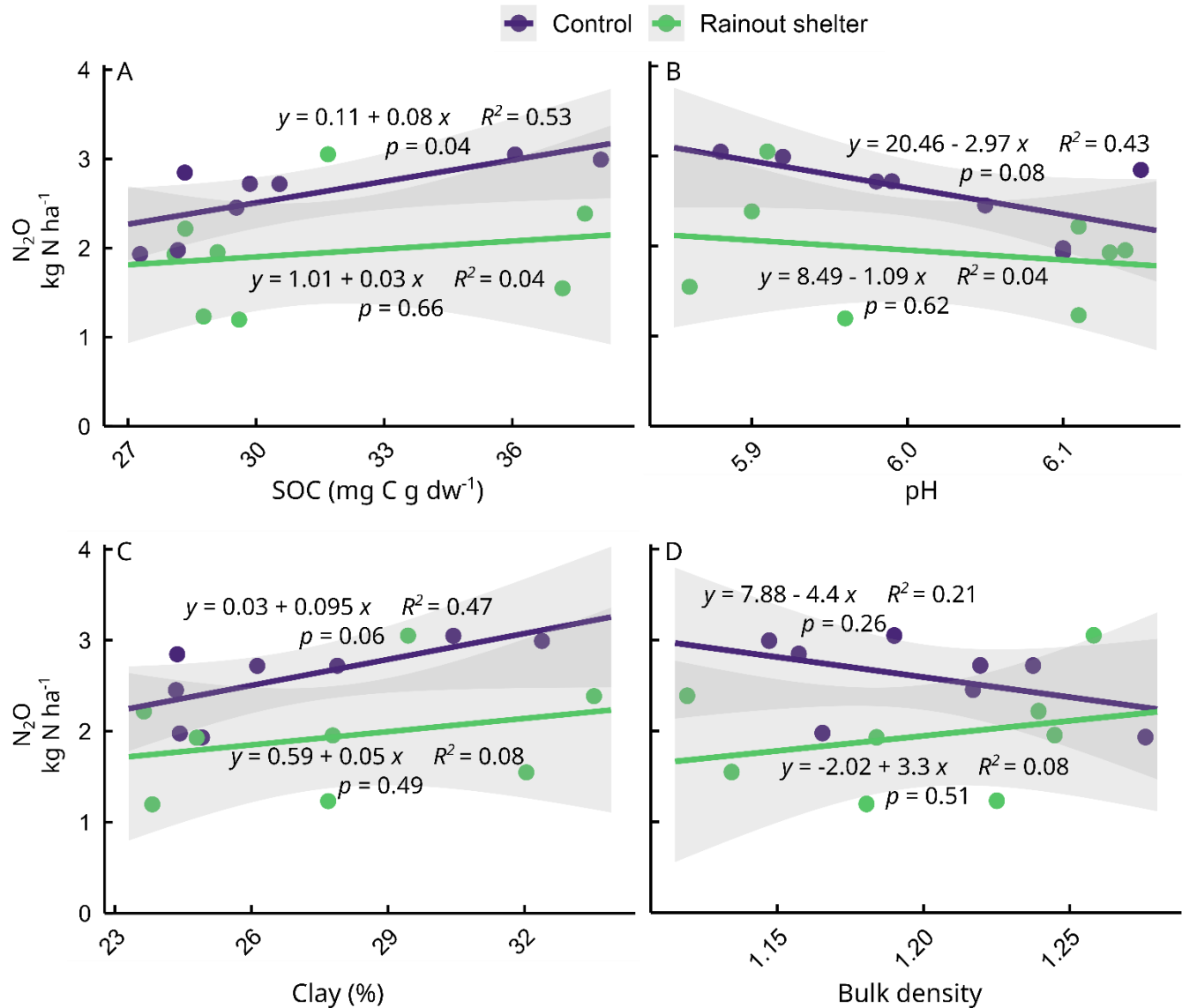


**Figure 6: Cumulative  $\text{N}_2\text{O}$  emissions as a function of (A) soil organic carbon (SOC) content, (B) pH, (C) clay content and (D) bulk density ( $\text{g cm}^{-3}$ ) during the second experimental year. Data are shown for control plots (purple) and rainout shelter plots (green). Solid lines are linear regression lines for control or rainout shelter plots with the shaded areas indicating 95% confidence intervals. The regression equations, coefficients of determination ( $R^2$ ) and  $p$ -values are displayed next to each regression line**



## 4 Discussion

### 4.1 Effect of reduced precipitation

Climate models predict that Norway, like much of northern Europe, will experience a warmer and wetter climate with more  
255 frequent and severe summer droughts (Wong et al., 2011; Hanssen-Bauer et al., 2017; Zhu and Siebert, 2024). The rainout  
shelters in our study effectively simulated these conditions by consistently reducing precipitation and soil moisture compared  
to the control plots, especially during the summer months (Fig. 2D and 1). However, during periods of heavy precipitation,  
soil moisture under the rainout shelters raised to levels comparable or above those in control plots. This resulted in a bimodal  
WFPS distribution in the rainout shelter plots (Fig. 1), which resembles the future climate with both more frequent low soil  
260 moistures due to drought and more frequent wet soils due to increased precipitation.

The effect of the rainout shelters on  $\text{N}_2\text{O}$  emissions differed between the two years. In the first year, average cumulative  $\text{N}_2\text{O}$   
emissions did not vary between control and rainout shelter plots (Fig. 4C). The rainout shelters were installed end of June,  
about two months after fertilisation, which likely limited mineral N availability. Still, high concentrations of mineral N were  
observed during this period, although this did not translate into higher  $\text{N}_2\text{O}$  emissions (Fig. 2B, C). Later in the first year,  
265 extreme precipitation events ( $> 40 \text{ mm day}^{-1}$ ; Fig. 2E) cancelled out differences in soil moisture between the control and  
rainout shelter plots (Fig. 2D). For example, the sixth rainout shelter from the hilltop (plot F; Table 2) had a similar median  
WFPS as its corresponding control plot, while the eighth rainout shelter (plot H; Table 2) had a higher median WFPS than its  
control plot during flux measurement periods (Fig. S3A). This resulted in no clear difference in  $\text{N}_2\text{O}$  emissions between  
control and rainout shelter in plot F and higher  $\text{N}_2\text{O}$  emissions in the rainout shelter plot H (Fig. 4A). Snow came early  
270 (October) in the first year, and we only measured  $\text{N}_2\text{O}$  for four months. We believe the combination of limited N availability  
during the growing season, heavy precipitation events in autumn and the short measurement period explains the absence of a  
consistent rainout effect on  $\text{N}_2\text{O}$  emissions in the first year.

In the second year, rainout shelters were installed earlier and were deployed for almost nine months, which likely resulted in  
a more sustained effect of precipitation reduction on soil processes. Average cumulative  $\text{N}_2\text{O}$  emissions were significantly  
275 larger in control plots (Fig. 4D), indicating that reduced precipitation decreased soil moisture, and thereby decreased  
denitrification and  $\text{N}_2\text{O}$  emissions. Consistent with the findings of our study, meta-analyses have shown that rainout shelters  
generally reduce  $\text{N}_2\text{O}$  emissions compared to ambient precipitation in field studies (Homyak et al., 2017; Li et al., 2020).  
The primary mechanism for this reduction is a decrease in the anoxic volume in the soil, which limits denitrification  
(Schlüter et al., 2025; Firestone et al., 1979). Larger  $\text{N}_2\text{O}$  emissions are commonly observed at WFPS values  $>60\%$ , as  
280 anoxic microsites become more prevalent, supporting denitrification (Davidson, 1993; Robertson and Groffman, 2007;  
Schlüter et al., 2025). Conversely, smaller  $\text{N}_2\text{O}$  emissions can be expected when soil moisture is low (WFPS  $<60\%$ ), as low  
soil moisture reduces the anoxic volume in the soil and limits diffusion of mineral N and organic C to microbes (Linn and  
Doran, 1984; Roman-Perez and Hernandez-Ramirez, 2021). This aligns well with our observation of more flux  
measurements at WFPS  $<60\%$  and hence smaller  $\text{N}_2\text{O}$  emissions in the rainout shelter plots, whereas control plots had more



285 frequent WFPS values >60% resulting in larger N<sub>2</sub>O emissions (Fig. 1B and 4D). Base N<sub>2</sub>O emissions, i.e. emissions measured outside periods of high-flux events, appeared to be generally higher in the control plots, displaying a larger interquartile range than emissions in the rainout shelter plots (Fig. 3C).

Plot-specific variability in WFPS and N<sub>2</sub>O emissions was observed also in the second year. For instance, in plot F, the rainout shelter plot had a lower median WFPS than the control plot, but the rainout shelter WFPS exhibited greater 290 variability, with some measured WFPS higher than in the control plot (Fig. S3B). This variability likely contributed to higher N<sub>2</sub>O emissions in the rainout shelter plot in periods with high WFPS. Despite such plot-level differences, the overall trend of reduced N<sub>2</sub>O emissions under rainout shelters was evident.

The reduced N<sub>2</sub>O emissions under rainout shelters, however, did not result in a climate benefit when considering the yield. Barley dry matter yield (DMY) exhibited high variability, and although we saw no significant difference between the control 295 and rainout shelter plots in either year, there was a trend towards lower yields in the rainout shelter plots (Fig. 5). In the second year, when the N<sub>2</sub>O measurement period was longer and more representative of the growing season, the average yield-scaled N<sub>2</sub>O emissions were not significantly different between the two treatments amounting to  $0.53 \pm 0.23$  and  $0.48 \pm 0.28$  kg N<sub>2</sub>O-N Mg DMY ha<sup>-1</sup> for the control and rainout shelter plots, respectively. Although the second year better represents growing season and post-harvest emissions, cumulative N<sub>2</sub>O emissions were likely underestimated, as only few 300 freeze-thaw cycles were captured in spring and most of the off-season was not included. Freeze-thaw cycles are known to contribute a large part of the annual emission in cool-temperate climates (Christensen and Tiedje, 1990; Flessa et al., 1995; Wagner-Riddle and Thurtell, 1998; Wagner-Riddle et al., 2024). At our experimental farm, a cover crop study on a neighbouring field found that 62–80% of the annual N<sub>2</sub>O emissions occurred during the off-season in plots without cover crops (Kjær et al., 2026b). Investigating how precipitation manipulation during the growing season affects the off-season 305 emissions was beyond the scope of the present study.

## 4.2 Impact of edaphic drivers

In addition to the dominant effect of precipitation, our results highlight the importance of soil physicochemical properties in driving N<sub>2</sub>O emissions when soil moisture is not limiting. In the second year, reduced precipitation not only lowered 310 cumulative N<sub>2</sub>O emissions but also diminished the influence of environmental drivers such as SOC, clay content and pH along the hillslope. This suggests that under drier conditions, limited soil moisture can suppress the effect of soil properties in regulating N<sub>2</sub>O fluxes.

While other studies have examined N<sub>2</sub>O emissions in relation to soil and climate variables across broad management and climate gradients (Jia et al., 2025; Hargreaves et al., 2021), our study offers insights into the effect of small-scale variability on the field level. Along the 62 metres of hillslope, we observed notable variation in SOC (27.3–38.1 mg C g<sup>-1</sup>), clay (24–315 34%) and pH (5.86–6.15), with SOC increasing downslope and correlating positively with clay content and negatively with pH.



SOC content is often considered a potential driver for  $\text{N}_2\text{O}$  emissions (Li et al., 2005; Stehfest and Bouwman, 2006) among others by creating anoxic microsites due to increased  $\text{O}_2$  consumption (Jäger et al., 2011). Particulate organic matter (POM) especially can create hotspots of increased microbial activity and  $\text{O}_2$  consumption resulting in enhanced denitrification in 320 otherwise oxic soil (Lucas et al., 2024; Schlüter et al., 2025; Surey et al., 2021). In our study, we found no relationship between POM and  $\text{N}_2\text{O}$  emissions for either ambient or reduced precipitation conditions ( $p = 0.86$  and  $p = 0.31$ , respectively; data not shown), suggesting that the positive correlation between SOC and  $\text{N}_2\text{O}$  was not driven by C availability.

A companion study using soil from the same plots identified clay content as the dominant factor controlling SOC stabilisation (Kjær et al., 2026a). Soils with higher clay content along the gradient had lower microbial respiration potentials 325 and stabilised more  $^{13}\text{C}$ -labelled litter into mineral associated organic matter (MAOM). Therefore, the availability of SOC was not higher in the high-SOC soils, refuting the idea that higher  $\text{N}_2\text{O}$  emissions in plots with higher SOC content were fuelled by SOC.

High SOC content is commonly associated with certain soil physicochemical properties, such as improved aggregation, gas 330 diffusivity and increased substrate availability, all of which are known to affect  $\text{N}_2\text{O}$  emissions in several, sometimes opposing, ways (Li et al., 2021; Six et al., 2002b; Kelley et al., 2024). For instance, poor soil aggregation may restrict  $\text{O}_2$  diffusion, potentially promoting denitrification and  $\text{N}_2\text{O}$  emissions under wet conditions. Conversely, better aggregation and protection of SOC in microaggregates limits the availability of labile C-substrates for microbes, thereby reducing  $\text{N}_2\text{O}$  fluxes (Sato et al., 2019). The multiple, partly adverse effects of SOC on  $\text{N}_2\text{O}$  make it difficult to pinpoint direct effects.

In our study, SOC and clay content were closely correlated, raising the possibility that the observed positive relationship 335 between SOC and  $\text{N}_2\text{O}$  was due to collinearity with clay content rather than a direct effect of SOC on  $\text{N}_2\text{O}$  turnover. High clay content is known to enhance soil water-holding capacity, creating anoxic microsites conducive to denitrification (Li et al., 2024; Keiluweit et al., 2018). Clay content may also promote  $\text{N}_2\text{O}$  emissions through interactions between soil texture and root exudates, which can create localised anoxic zones (Lacroix et al., 2025). However, we did not see an increase in volumetric water content at field capacity with increasing SOC or clay (Table 2), which may be due to the fine texture of our 340 soils (Minasny and Mcbratney, 2018).

Both SOC and clay content were negatively correlated with pH, and a near-significant relationship was observed between pH and  $\text{N}_2\text{O}$  emissions. A field study from southeastern Norway found that pH, rather than SOC, was the dominant factor controlling  $\text{N}_2\text{O}$  emissions during the off-season (Russenes et al., 2016). This suggests that pH modulates *in situ*  $\text{N}_2\text{O}$  emissions, although its effect is intertwined with SOC and clay content. The decline in pH downslope may be due to the 345 accumulation or production of organic acids (Adeleke et al., 2017), which can be influenced by both SOC and clay content. This interconnectedness indicates that even if pH appears to be a dominant factor controlling  $\text{N}_2\text{O}$  emissions, its effects are modulated by SOC and clay content, making it impossible to fully separate their contributions. In summary, while SOC, clay and pH each showed some degree of influence on cumulative  $\text{N}_2\text{O}$  emissions, their effects were secondary to the impact of precipitation reduction which appeared to be the dominant factor. Despite the confounding effect of edaphic factors, the



350 observed trends in our small-scale study highlight the importance of considering local soil variability when assessing N<sub>2</sub>O emissions in agricultural systems.

The most striking finding of our study was that the influence of physicochemical variables on cumulative N<sub>2</sub>O emissions changed markedly with precipitation regime in the second year. While it is well established that soil N<sub>2</sub>O emissions depend on soil moisture, our rainout shelter experiment demonstrated that manipulating precipitation not only reduced cumulative 355 N<sub>2</sub>O emissions (by ~25%), but also effectively cancelled out the relationships between N<sub>2</sub>O emissions and SOC content, clay content and pH that were evident under ambient precipitation. The shift in soil moisture distribution towards more frequent WFPS values between 35 and 50% (Fig. 1) likely constrained the range of conditions under which these soil properties exert an effect.

This phenomenon could be explained by a shift in prevailing soil moisture altering the dominant N<sub>2</sub>O production process, 360 each with distinct sensitivities to SOC, clay and pH. For instance, nitrification and its N<sub>2</sub>O yield are known to be positively related to soil pH (Nadeem et al., 2020) potentially cancelling out the well-known negative relationship between the N<sub>2</sub>O product ratio of denitrification and pH (Bergaust et al., 2010). Additionally, the edaphic gradient may have given raise to distinct microbial communities that respond differently to changes in soil moisture. In our companion study (Kjær et al., 2026a) we found that the abundance of *nosZ* was negatively correlated with SOC along the studied gradient ( $p < 0.01$ ) 365 indicating a higher potential for complete denitrification at the top of the hillslope. Rain exclusion may have weakened this control by shifting the soil towards nitrifying conditions.

Most process-based models are limited in capturing dynamic interactions between soil physicochemical and soil moisture controls on N<sub>2</sub>O emissions. Our findings highlight that the influence of SOC, clay content and pH on N<sub>2</sub>O emissions can be strongly conditional and are easily cancelled out by changes in precipitation regime. This context-dependency presents a 370 challenge for model parameterisation, as relationships derived under one set of moisture conditions may not be transferable to others.

## 5 Conclusion

This study demonstrates that reduced precipitation limits cumulative N<sub>2</sub>O emissions by decreasing soil moisture, likely 375 resulting in less denitrification. We found that reduced precipitation overrode well-known physicochemical controls of N<sub>2</sub>O emissions observed under ambient conditions. While soil physicochemical controls on N<sub>2</sub>O emissions at small scales are difficult to disentangle, these properties likely interact to shape N-dynamics and control N<sub>2</sub>O emissions when soil moisture is not limiting. The observed trends suggest that small-scale soil variability plays an important role in regulating N<sub>2</sub>O emissions, but only when precipitation is sufficient to allow denitrification to be the dominant N<sub>2</sub>O source. Overall, our 380 findings emphasise the dominant role of precipitation in controlling N<sub>2</sub>O emissions in cool-humid crop production, which is particularly relevant as future climate scenarios predict changes in rainfall patterns and the occurrence of droughts.



## Data availability

Data and code are available at <https://doi.org/10.5281/zenodo.18173363>.

## 385 Author contributions

**Sigrid Trier Kjær:** Conceptualisation, Data curation, Formal analysis, Investigation, Visualisation, Writing – original draft, Writing – review & editing. **Peter Dörsch:** Conceptualisation, Funding acquisition, Supervision, Writing – review & editing.

## Declaration of generative AI and AI-assisted technologies

During the preparation of this work, ChatGPT (GPT-4; OpenAI) was used to improve readability and language in the  
390 manuscript and for data handling by writing code for R. All output from the AI tool were quality checked and revised by authors before going into the manuscript.

## Competing interests

The authors declare that they have no conflict of interest.

## Acknowledgements

395 We would like to thank Trygve Fredriksen, Øyvind Peder Vartdal and Elias Rogstad for their valuable assistance in field and laboratory work. Sigrid would also like to thank Lena Bakker and Eliane Schmid for support and writing huddles.

## Financial support

This work was supported by TRUESOIL, a project funded by the 1<sup>st</sup> external call from the European Joint Programme EJP SOIL (Horizon 2020: 862695), with funding from the Research Council of Norway (Project number 336692).

## 400 References

Adeleke, R., Nwangburuka, C., and Oboirien, B.: Origins, roles and fate of organic acids in soils: A review, South African Journal of Botany, 108, 393-406, <https://doi.org/10.1016/j.sajb.2016.09.002>, 2017.



Bakken, L. R., Bergaust, L., Liu, B., and Frostegård, Å.: Regulation of denitrification at the cellular level: a clue to the understanding of N<sub>2</sub>O emissions from soils, *Philosophical Transactions of the Royal Society B: Biological Sciences*, 367, 405 1226-1234, <https://doi.org/10.1098/rstb.2011.0321>, 2012.

Barrat, H. A., Evans, J., Chadwick, D. R., Clark, I. M., Le Cocq, K., and M. Cardenas, L.: The impact of drought and rewetting on N<sub>2</sub>O emissions from soil in temperate and Mediterranean climates, *European Journal of Soil Science*, 72, 2504-2516, <https://doi.org/10.1111/ejss.13015>, 2021.

Bergaust, L., Mao, Y., Bakken Lars, R., and Frostegård, Å.: Denitrification Response Patterns during the Transition to 410 Anoxic Respiration and Posttranscriptional Effects of Suboptimal pH on Nitrogen Oxide Reductase in *Paracoccus denitrificans*, *Appl Environ Microbiol*, 76, 6387-6396, <https://doi.org/10.1128/AEM.00608-10>, 2010.

Borken, W. and Matzner, E.: Reappraisal of drying and wetting effects on C and N mineralization and fluxes in soils, *Global Change Biology*, 15, 808-824, <https://doi.org/10.1111/j.1365-2486.2008.01681.x>, 2009.

Butterbach-Bahl, K., Baggs, E. M., Dannenmann, M., Kiese, R., and Zechmeister-Boltenstern, S.: Nitrous oxide emissions 415 from soils: how well do we understand the processes and their controls?, *Philosophical Transactions of the Royal Society B: Biological Sciences*, 368, 20130122, <https://doi.org/10.1098/rstb.2013.0122>, 2013.

Christensen, S. and Tiedje, J. M.: Brief and vigorous N<sub>2</sub>O production by soil at spring thaw, *Journal of Soil Science*, 41, 1-4, 420 <https://doi.org/10.1111/j.1365-2389.1990.tb00039.x>, 1990.

Davidson, E. A.: Soil Water Content and the Ratio of Nitrous Oxide to Nitric Oxide Emitted from Soil, in: *Biogeochemistry of Global Change: Radiatively Active Trace Gases Selected Papers from the Tenth International Symposium on Environmental Biogeochemistry*, San Francisco, August 19–24, 1991, edited by: Oremland, R. S., Springer US, Boston, MA, 369-386, [https://doi.org/10.1007/978-1-4615-2812-8\\_20](https://doi.org/10.1007/978-1-4615-2812-8_20), 1993.

Doane, T. A. and Horwáth, W. R.: Spectrophotometric Determination of Nitrate with a Single Reagent, *Analytical Letters*, 36, 2713-2722, <https://doi.org/10.1081/AL-120024647>, 2003.

425 Elonen, P.: Particle-size analysis of soil, *Acta Agralia Fennica*, 122, 1-122, 1971.

Firestone, M. K.: Biological Denitrification, in: *Nitrogen in Agricultural Soils*, *Agronomy Monographs*, 289-326, <https://doi.org/10.2134/agronmonogr22.c8>, 1982.

Firestone, M. K., Smith, M. S., Firestone, R. B., and Tiedje, J. M.: The Influence of Nitrate, Nitrite, and Oxygen on the 430 Composition of the Gaseous Products of Denitrification in Soil, *Soil Science Society of America Journal*, 43, 1140-1144, <https://doi.org/10.2136/sssaj1979.03615995004300060016x>, 1979.

Flessa, H., Dörsch, P., and Beese, F.: Seasonal variation of N<sub>2</sub>O and CH<sub>4</sub> fluxes in differently managed arable soils in southern Germany, *Journal of Geophysical Research: Atmospheres*, 100, 23115-23124, <https://doi.org/10.1029/95JD02270>, 1995.

435 Ge, X., Xie, D., Mulder, J., and Duan, L.: Reevaluating the Drivers of Fertilizer-Induced N<sub>2</sub>O Emission: Insights from Interpretable Machine Learning, *Environmental Science & Technology*, 58, 15672-15680, <https://doi.org/10.1021/acs.est.4c04574>, 2024.



Hanssen-Bauer, I., Førland, E. J., Haddeland, I., Hisdal, H., Lawrence, D., Mayer, S., Nesje, A., Nilsen, J. E. Ø., Sandven, S., Sandø, A. B., Sorteberg, A., and Ådlandsvik, B.: Climate in Norway 2100 – a knowledge base for climate adaptation, Norwegian Environment Agency (Miljødirektoratet), 2017.

440 Hargreaves, P. R., Baker, K. L., Graceson, A., Bonnett, S. A. F., Ball, B. C., and Cloy, J. M.: Use of a nitrification inhibitor reduces nitrous oxide (N<sub>2</sub>O) emissions from compacted grassland with different soil textures and climatic conditions, *Agriculture, Ecosystems & Environment*, 310, 107307, <https://doi.org/10.1016/j.agee.2021.107307>, 2021.

Harrison-Kirk, T., Beare, M. H., Meenken, E. D., and Condron, L. M.: Soil organic matter and texture affect responses to dry/wet cycles: Effects on carbon dioxide and nitrous oxide emissions, *Soil Biology and Biochemistry*, 57, 43-55,

445 <https://doi.org/10.1016/j.soilbio.2012.10.008>, 2013.

Hartmann, A. A. and Niklaus, P. A.: Effects of simulated drought and nitrogen fertilizer on plant productivity and nitrous oxide (N<sub>2</sub>O) emissions of two pastures, *Plant and Soil*, 361, 411-426, <https://doi.org/10.1007/s11104-012-1248-x>, 2012.

Homyak, P. M., Allison, S. D., Huxman, T. E., Goulden, M. L., and Treseder, K. K.: Effects of Drought Manipulation on Soil Nitrogen Cycling: A Meta-Analysis, *Journal of Geophysical Research: Biogeosciences*, 122, 3260-3272,

450 <https://doi.org/10.1002/2017JG004146>, 2017.

IPCC, Nabuurs, G.-J., Mrabet, R., Abu Hatab, A., Bustamante, M., Clark, H., Havlík, P., House, J., Mbow, C., Ninan, K. N., Popp, A., Roe, S., Sohngen, B., and Towprayoon, S.: Agriculture, Forestry and Other Land Uses (AFOLU), in: IPCC 2022: Climate Change 2022: Mitigation of Climate Change: Working Group III Contribution to the Sixth Assessment Report of the Intergovernmental Panel on Climate Change, edited by: Intergovernmental Panel on Climate, C., Cambridge University Press, Cambridge, UK and New York, NY, USA, 747-860, <https://doi.org/10.1017/9781009157926.009>, 2023.

Jäger, N., Stange, C. F., Ludwig, B., and Flessa, H.: Emission rates of N<sub>2</sub>O and CO<sub>2</sub> from soils with different organic matter content from three long-term fertilization experiments—a laboratory study, *Biology and Fertility of Soils*, 47, 483-494, <https://doi.org/10.1007/s00374-011-0553-5>, 2011.

Jia, L., Yang, H., Li, Y., Du, Z., Ju, X., Li, Y., and Wu, D.: Soil clay content determined the temperature response of N<sub>2</sub>O emissions derived from denitrification, *Applied Soil Ecology*, 216, 106500, <https://doi.org/10.1016/j.apsoil.2025.106500>, 2025.

Kaiser, E. A., Eiland, F., Germon, J. C., Gispert, M. A., Heinemeyer, O., Henault, C., Lind, A. M., Maag, M., Saguer, E., Van Cleemput, O., Vermoesen, A., and Webster, C.: What predicts nitrous oxide emissions and denitrification N-loss from European soils?, *Zeitschrift für Pflanzenernährung und Bodenkunde*, 159, 541-547,

465 <https://doi.org/10.1002/jpln.1996.3581590604>, 1996.

Keiluweit, M., Gee, K., Denney, A., and Fendorf, S.: Anoxic microsites in upland soils dominantly controlled by clay content, *Soil Biology and Biochemistry*, 118, 42-50, <https://doi.org/10.1016/j.soilbio.2017.12.002>, 2018.

Kelley, L. A., Zhang, Z., Tamagno, S., Lundy, M. E., Mitchell, J. P., Gaudin, A. C. M., and Pittelkow, C. M.: Changes in soil N<sub>2</sub>O emissions and nitrogen use efficiency following long-term soil carbon storage: Evidence from a mesocosm experiment, *Agriculture, Ecosystems & Environment*, 370, 109054, <https://doi.org/10.1016/j.agee.2024.109054>, 2024.



Kjær, S. T., Bogdanov, K., Morales, S. E., Dörsch, P.: Clay content, not microbial community composition, regulates carbon stabilisation along a soil carbon and texture gradient impacted by reduced precipitation, SSRN [preprint], <https://ssrn.com/abstract=6071988>, 14 January 2026a.

475 Kjær, S. T., Lang, R., Kätterer, T., and Dörsch, P.: Species specific effects of cover crops on nitrous oxide emissions in hemiboreal cereal production: The importance of freeze-thaw driven emissions, *Agriculture, Ecosystems & Environment*, 397, 110061, <https://doi.org/10.1016/j.agee.2025.110061>, 2026b.

Krogstad, T., Jørgensen, P., Sogn, T., Børresen, T., and Kolnes, A. G.: Manual for kornfordelingsanalyse etter pipettemetoden. Forbehandling og pipetteprosedyre. Dataprogrammer for veiling, beregning og utskrift., Institutt for Jordfag 1991.

480 Krom, M. D.: Spectrophotometric determination of ammonia: a study of a modified Berthelot reaction using salicylate and dichloroisocyanurate, *Analyst*, 105, 305-316, <http://dx.doi.org/10.1039/an9800500305>, 1980.

Kundel, D., Meyer, S., Birkhofer, H., Fliessbach, A., Mäder, P., Scheu, S., van Kleunen, M., and Birkhofer, K.: Design and Manual to Construct Rainout-Shelters for Climate Change Experiments in Agroecosystems, *Frontiers in Environmental Science*, 6, <https://doi.org/10.3389/fenvs.2018.00014>, 2018.

485 Lacroix, E. M., Frei, J., van der Loo, E., Kocsis, L., and Keiluweit, M.: Root exudation and fine texture interact to form anoxic microsites in rhizosphere soil, *Soil Biology and Biochemistry*, 211, 109974, <https://doi.org/10.1016/j.soilbio.2025.109974>, 2025.

490 Li, C., Frolking, S., and Butterbach-Bahl, K.: Carbon Sequestration in Arable Soils is Likely to Increase Nitrous Oxide Emissions, Offsetting Reductions in Climate Radiative Forcing, *Climatic Change*, 72, 321-338, <https://doi.org/10.1007/s10584-005-6791-5>, 2005.

Li, L., Hong, M., Zhang, Y., and Paustian, K.: Soil N<sub>2</sub>O emissions from specialty crop systems: A global estimation and meta-analysis, *Global Change Biology*, 30, e17233, <https://doi.org/10.1111/gcb.17233>, 2024.

495 Li, L., Zheng, Z., Wang, W., Biederman, J. A., Xu, X., Ran, Q., Qian, R., Xu, C., Zhang, B., Wang, F., Zhou, S., Cui, L., Che, R., Hao, Y., Cui, X., Xu, Z., and Wang, Y.: Terrestrial N<sub>2</sub>O emissions and related functional genes under climate change: A global meta-analysis, *Global Change Biology*, 26, 931-943, <https://doi.org/10.1111/gcb.14847>, 2020.

Li, Y., Clough, T. J., Moinet, G. Y. K., and Whitehead, D.: Emissions of nitrous oxide, dinitrogen and carbon dioxide from three soils amended with carbon substrates under varying soil matric potentials, *European Journal of Soil Science*, 72, 2261-2275, <https://doi.org/10.1111/ejss.13124>, 2021.

500 Linn, D. M. and Doran, J. W.: Effect of Water-Filled Pore Space on Carbon Dioxide and Nitrous Oxide Production in Tilled and Nontilled Soils, *Soil Science Society of America Journal*, 48, 1267-1272, <https://doi.org/10.2136/sssaj1984.03615995004800060013x>, 1984.

Lucas, M., Rohe, L., Apelt, B., Stange, C. F., Vogel, H.-J., Well, R., and Schlüter, S.: The distribution of particulate organic matter in the heterogeneous soil matrix - Balancing between aerobic respiration and denitrification, *Science of The Total Environment*, 951, 175383, <https://doi.org/10.1016/j.scitotenv.2024.175383>, 2024.



505 Minasny, B. and McBratney, A. B.: Limited effect of organic matter on soil available water capacity, European Journal of Soil Science, 69, 39-47, <https://doi.org/10.1111/ejss.12475>, 2018.

Nadeem, S., Bakken, L. R., Frostegård, Å., Gaby, J. C., and Dörsch, P.: Contingent Effects of Liming on N<sub>2</sub>O-Emissions Driven by Autotrophic Nitrification, Frontiers in Environmental Science, Volume 8 - 2020, <https://doi.org/10.3389/fenvs.2020.598513>, 2020.

510 Nemes, A., Rawls, W. J., and Pachepsky, Y. A.: Influence of Organic Matter on the Estimation of Saturated Hydraulic Conductivity, Soil Science Society of America Journal, 69, 1330-1337, <https://doi.org/10.2136/sssaj2004.0055>, 2005.

Pihlatie, M., Syväsalo, E., Simojoki, A., Esala, M., and Regina, K.: Contribution of nitrification and denitrification to N<sub>2</sub>O production in peat, clay and loamy sand soils under different soil moisture conditions, Nutrient Cycling in Agroecosystems, 70, 135-141, <https://doi.org/10.1023/B:FRES.0000048475.81211.3c>, 2004.

515 Ravishankara, A. R., Daniel, J. S., and Portmann, R. W.: Nitrous Oxide (N<sub>2</sub>O): The Dominant Ozone-Depleting Substance Emitted in the 21st Century, Science, 326, 123-125, <https://doi.org/10.1126/science.1176985>, 2009.

Robertson, G. P. and Groffman, P. M.: 13 - NITROGEN TRANSFORMATIONS, in: Soil Microbiology, Ecology and Biochemistry (Third Edition), edited by: Paul, E. A., Academic Press, San Diego, 341-364, <https://doi.org/10.1016/B978-0-08-047514-1.50017-2>, 2007.

520 Roman-Perez, C. C. and Hernandez-Ramirez, G.: Sources and priming of nitrous oxide production across a range of moisture contents in a soil with high organic matter, Journal of Environmental Quality, 50, 94-109, <https://doi.org/10.1002/jeq2.20172>, 2021.

Rummel, P. S., Pfeiffer, B., Pausch, J., Well, R., Schneider, D., and Ditttert, K.: Maize root and shoot litter quality controls short-term CO<sub>2</sub> and N<sub>2</sub>O emissions and bacterial community structure of arable soil, Biogeosciences, 17, 1181-1198, <https://doi.org/10.5194/bg-17-1181-2020>, 2020.

525 Russenes, A. L., Korsaeth, A., Bakken, L. R., and Dörsch, P.: Spatial variation in soil pH controls off-season N<sub>2</sub>O emission in an agricultural soil, Soil Biology and Biochemistry, 99, 36-46, <https://doi.org/10.1016/j.soilbio.2016.04.019>, 2016.

Sato, J. H., de Figueiredo, C. C., Marchão, R. L., de Oliveira, A. D., Vilela, L., Delvico, F. M., Alves, B. J. R., and de Carvalho, A. M.: Understanding the relations between soil organic matter fractions and N<sub>2</sub>O emissions in a long-term integrated crop–livestock system, European Journal of Soil Science, 70, 1183-1196, <https://doi.org/10.1111/ejss.12819>, 2019.

530 Schlüter, S., Lucas, M., Grosz, B., Ippisch, O., Zawallich, J., He, H., Dechow, R., Kraus, D., Blagodatsky, S., Senbayram, M., Kravchenko, A., Vogel, H.-J., and Well, R.: The anaerobic soil volume as a controlling factor of denitrification: a review, Biology and Fertility of Soils, 61, 343-365, <https://doi.org/10.1007/s00374-024-01819-8>, 2025.

535 Area Under the Curve: <https://search.r-project.org/CRAN/refmans/DescTools/html/AUC.html>, last access: 7th of January 2026.

Six, J., Conant, R. T., Paul, E. A., and Paustian, K.: Stabilization mechanisms of soil organic matter: Implications for C-saturation of soils, Plant and Soil, 241, 155-176, <https://doi.org/10.1023/A:1016125726789>, 2002a.



540 Six, J., Feller, C., Denef, K., Ogle, S. M., Sa, J. C. d. M., and Albrecht, A.: Soil organic matter, biota and aggregation in temperate and tropical soils - Effects of no-tillage, *Agronomie*, 22, 755-775, 1 <https://doi.org/10.1051/agro:2002043>, 2002b.

545 Stehfest, E. and Bouwman, L.: N<sub>2</sub>O and NO emission from agricultural fields and soils under natural vegetation: summarizing available measurement data and modeling of global annual emissions, *Nutrient Cycling in Agroecosystems*, 74, 207-228, <https://doi.org/10.1007/s10705-006-9000-7>, 2006.

550 Stevens, R. J., Laughlin, R. J., and Malone, J. P.: Soil pH affects the processes reducing nitrate to nitrous oxide and di-nitrogen, *Soil Biology and Biochemistry*, 30, 1119-1126, [https://doi.org/10.1016/S0038-0717\(97\)00227-7](https://doi.org/10.1016/S0038-0717(97)00227-7), 1998.

555 Surey, R., Kaiser, K., Schimpf, C. M., Mueller, C. W., Böttcher, J., and Mikutta, R.: Contribution of Particulate and Mineral-Associated Organic Matter to Potential Denitrification of Agricultural Soils, *Frontiers in Environmental Science*, 9, <https://doi.org/10.3389/fenvs.2021.640534>, 2021.

560 R Core Team: R: A Language and Environment for Statistical Computing, R Foundation for Statistical Computing, 2025.

565 Tian, H., Xu, R., Canadell, J. G., Thompson, R. L., Winiwarter, W., Suntharalingam, P., Davidson, E. A., Ciais, P., Jackson, R. B., Janssens-Maenhout, G., Prather, M. J., Regnier, P., Pan, N., Pan, S., Peters, G. P., Shi, H., Tubiello, F. N., Zaehle, S., Zhou, F., Arneth, A., Battaglia, G., Berthet, S., Bopp, L., Bouwman, A. F., Buitenhuis, E. T., Chang, J., Chipperfield, M. P., Dangal, S. R. S., Dlugokencky, E., Elkins, J. W., Eyre, B. D., Fu, B., Hall, B., Ito, A., Joos, F., Krummel, P. B., Landolfi, A., Laruelle, G. G., Lauerwald, R., Li, W., Lienert, S., Maavara, T., MacLeod, M., Millet, D. B., Olin, S., Patra, P. K., Prinn, R. G., Raymond, P. A., Ruiz, D. J., van der Werf, G. R., Vuichard, N., Wang, J., Weiss, R. F., Wells, K. C., Wilson, C., Yang, J., and Yao, Y.: A comprehensive quantification of global nitrous oxide sources and sinks, *Nature*, 586, 248-256, <https://doi.org/10.1038/s41586-020-2780-0>, 2020.

570 Wagner-Riddle, C. and Thurtell, G. W.: Nitrous oxide emissions from agricultural fields during winter and spring thaw as affected by management practices, *Nutrient Cycling in Agroecosystems*, 52, 151-163, <https://doi.org/10.1023/A:1009788411566>, 1998.

575 Wolff, M.: Meteorologiske data for Ås 2024, in, Faculty of Science and Technology, The Norwegian University of Life Sciences Field station for bioclimatic studies, South Ås, 2025.

580 Wolff, M. and Grimenes, A. A.: Meteorologiske data for Ås 2023, in, Faculty of Science and Technology, The Norwegian University of Life Sciences Field station for bioclimatic studies, South Ås, 2024.

585 Wong, W. K., Beldring, S., Engen-Skaugen, T., Haddeland, I., and Hisdal, H.: Climate Change Effects on Spatiotemporal Patterns of Hydroclimatological Summer Droughts in Norway, *Journal of Hydrometeorology*, 12, 1205-1220, <https://doi.org/10.1175/2011JHM1357.1>, 2011.



Wu, Q., Yue, K., Ma, Y., Heděnec, P., Cai, Y., Chen, J., Zhang, H., Shao, J., Chang, S. X., and Li, Y.: Contrasting effects of altered precipitation regimes on soil nitrogen cycling at the global scale, *Global Change Biology*, 28, 6679-6695, <https://doi.org/10.1111/gcb.16392>, 2022.

Yang, J., Jia, X., Ma, H., Chen, X., Liu, J., Shangguan, Z., and Yan, W.: Effects of warming and precipitation changes on  
575 soil GHG fluxes: A meta-analysis, *Science of The Total Environment*, 827, 154351,  
<https://doi.org/10.1016/j.scitotenv.2022.154351>, 2022.

Yu, Y., Zhao, C., Zheng, N., Jia, H., and Yao, H.: Interactive effects of soil texture and salinity on nitrous oxide emissions following crop residue amendment, *Geoderma*, 337, 1146-1154, <https://doi.org/10.1016/j.geoderma.2018.11.012>, 2019.

Zhu, W. and Siebert, S.: Climate-driven interannual variability in subnational irrigation areas across Europe,  
580 *Communications Earth & Environment*, 5, 554, <https://doi.org/10.1038/s43247-024-01721-z>, 2024.